Supporting Information

Pt nanoparticles embedded metal-organic frameworks nanosheets for efficient alkaline hydrogen evolution

Guoxiang Chen,[a] Zhe Zhao, [a,b] Hong Zhu, [a] Alexander Solovev, [a,c]* Gaoshan Huang, [a,c,d]* and Yongfeng Mei [a,b,c,d]

[a] Department of Materials Science & State Key Laboratory of Molecular Engineering of Polymers, Fudan University, Shanghai 200438, P. R. China

[b] Shanghai Frontiers Science Research Base of Intelligent Optoelectronics and Perception Shanghai 200438, P. R. China

[c] International Institute of Intelligent Nanorobots and Nanosystems Shanghai 200438, P. R. China

[d] Yiwu Research Institute of Fudan University Yiwu, Zhejiang 322000, P. R. China

Corresponding authors:

E-mail address: solovev@fudan.edu.cn; gshuang@fudan.edu.cn

A. Materials, Synthesis, and Preparation Details

A.1: Chemicals and Materials

Hexachloroplatinic acid hexahydrate ($H_2PtCl_6 \cdot 6H_2O$, ≥ 99.9%) was purchased from Sigma-Aldrich. Nickel nitrate hexahydrate ($Ni(NO_3)_2 \cdot 6H_2O$, ≥ 99.9%) and Nafion (5 wt.%) were purchased from Aladdin Ltd. Pt/C catalyst (20 wt.% platinum on carbon black) was purchased from Alfa Aesar. *N, N*-Dimethylformamide (DMF, 99%), potassium hydroxide (KOH, ≥ 85.0%), and terephthalic acid were purchased from Sinapharm. The chemicals were used without further purification. Deionized (DI) water obtained from an ultra-pure water system was used in all experiments.

A.2: Synthesis of Ni-MOF-P

$Ni(NO_3)_2 \cdot 6H_2O$ (0.288 g) and PTA (0.496 g) were dissolved in the DMF (30 mL) under vigorous ultrasonication to form a uniform solution. Then, the beaker was sealed at 150 °C for 24 h in an oven. After cooling down to room temperature, the precipitates were washed with ethanol for three times and then collected by centrifugation at 3000 rpm for 15 min. The sample was subsequently dried in a vacuum at 60 °C for 12 h.

A.3: Characterization

The morphologies and microstructures of the as-prepared samples were characterized by field-emission scanning electron microscope (SEM, Nova NanoSem 450), transmission electron microscope, and high resolution transmission electron microscope (TEM/HRTEM, FEI Tecnai G2 F20 S-Twin). The energy disperse spectroscopy (EDS, Oxford X-Max 80T) was used to analyze the elements distribution of the samples. X-ray diffraction (XRD) was performed on a D8 ADVANCE X-ray diffractometer with Cu Ka radiation (λ = 1.5406 Å) to study the crystal structure of the samples. X-ray photoelectron spectroscopy (XPS) was performed on an Axis Ultra DLD spectrometer with a Mg Ka radiation source. ICP-OES was performed on Agilent 720ES. The thermogravimetric analysis (TGA) was performed on PerkinElmer TGA8000 with a heating rate of 6 °C/min in the air atmosphere.

B. Additional Results:

B.1.: SEM image of NF

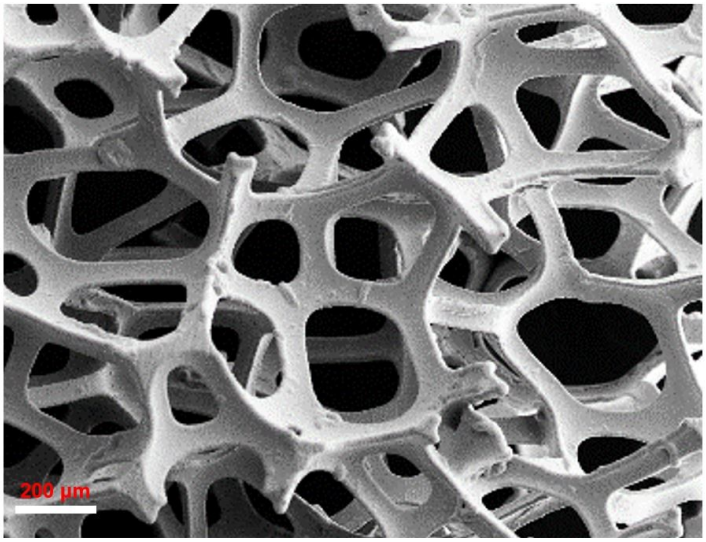

Figure S1: SEM image of bare NF.

B.2.: TEM image of Pt nanoparticles cluster

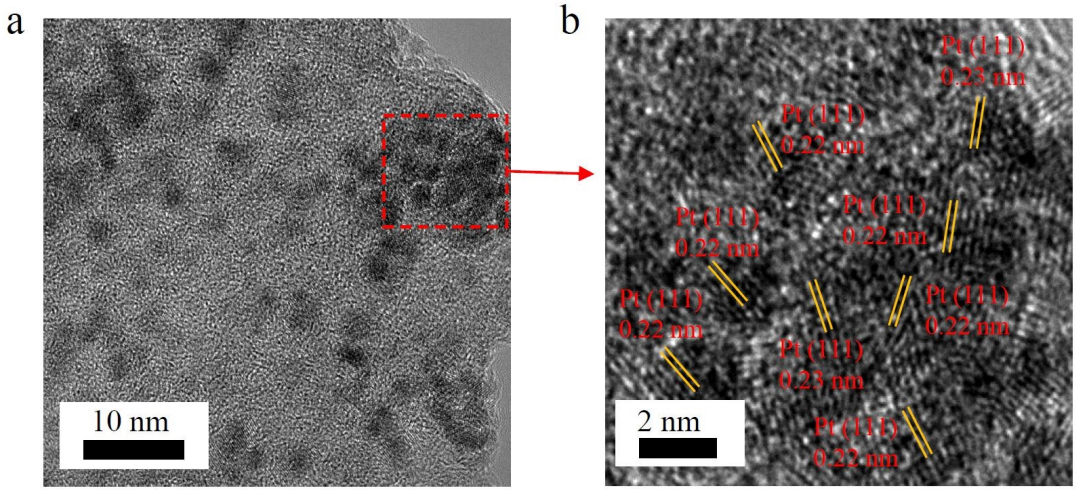

Figure S2: (a)TEM and (b) HRTEM images of the NF-MOF@Pt.

B.3.: SEM images of Ni-MOF-P

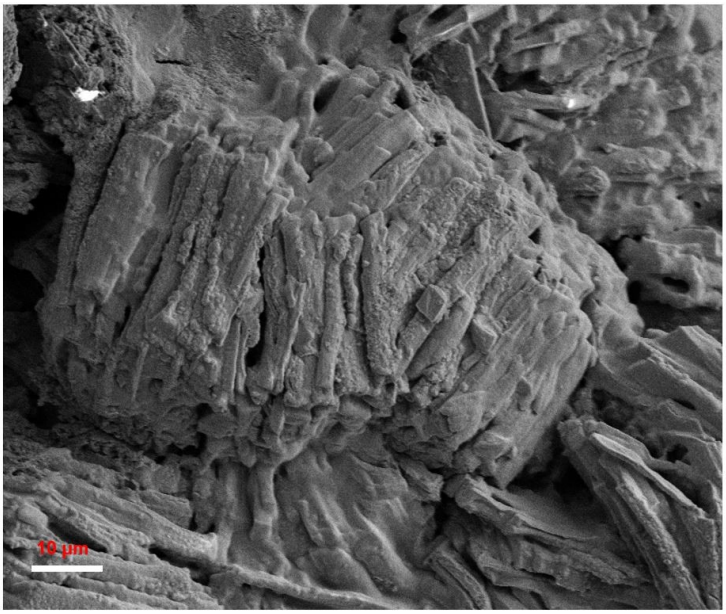

Figure S3: SEM images of Ni-MOF powder (Ni-MOF-P).

B.4.: XPS spectra of Ni 2p region for Ni-MOF-P and NF-MOF@Pt

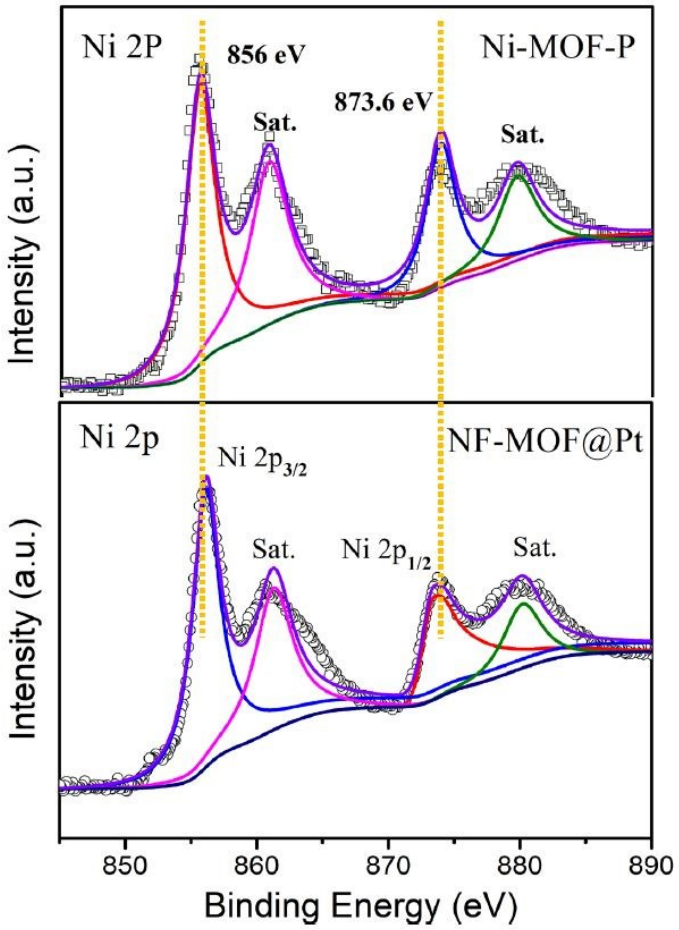

Figure S4: XPS spectra of Ni 2p region for Ni-MOF-P and NF-MOF@Pt.

B.5.: The XPS spectra of C in the NF-MOF@Pt composite

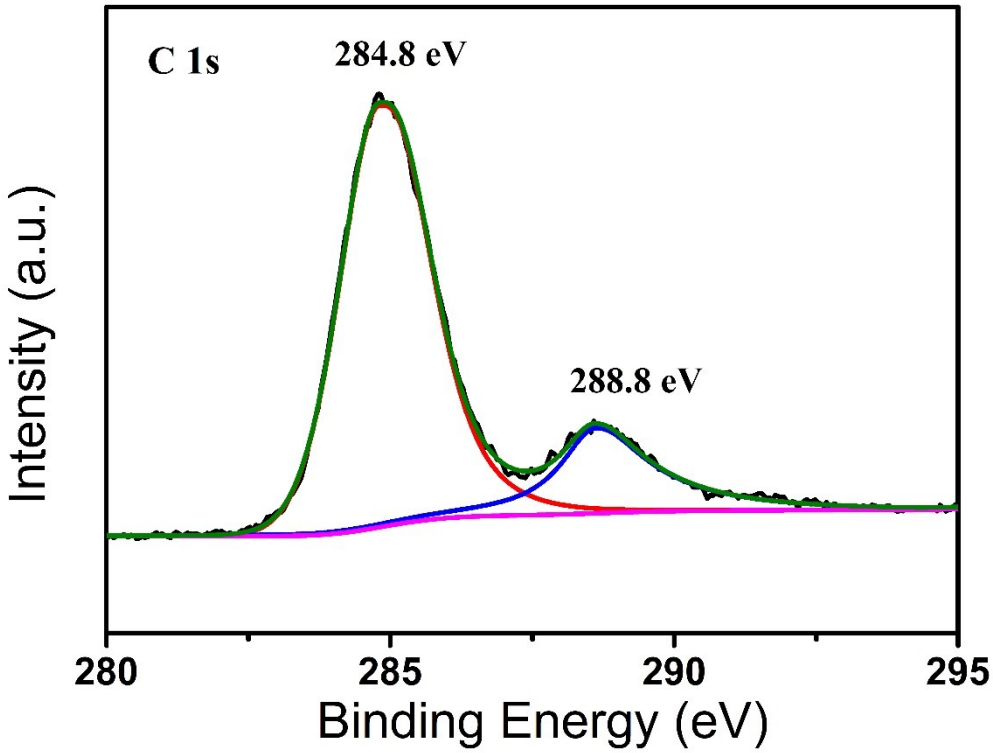

Figure S5: The high-resolution XPS spectra for C 1s.

B.6.: The EDS spectrum of NF-MOF@Pt

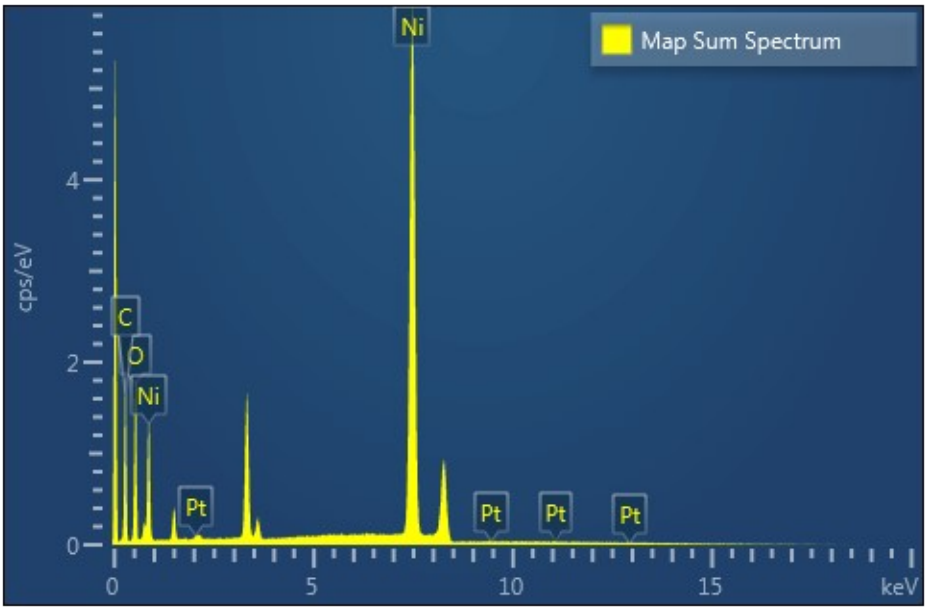

Figure S6: EDS spectrum of NF-MOF @Pt.

B.7.: LSV curves of NF-MOF@Pt with various Pt loadings

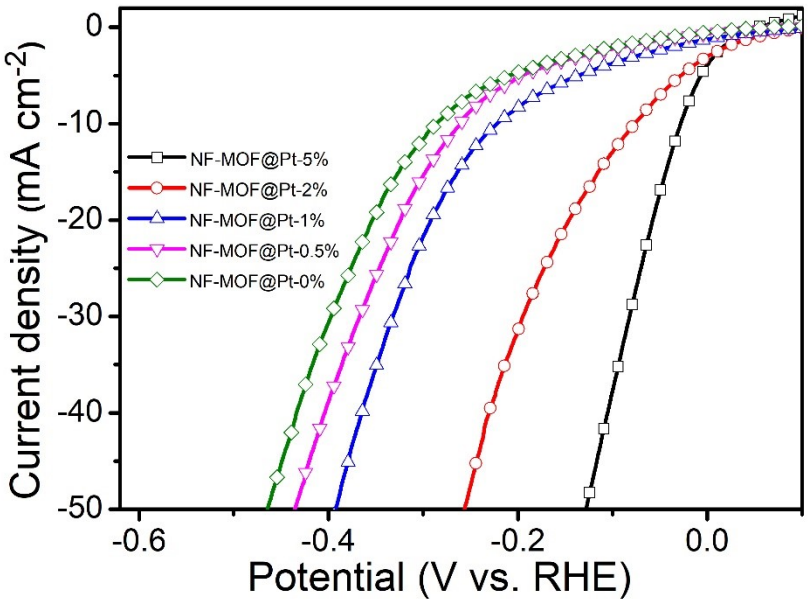

Figure S7: LSV curves of NF-MOF@Pt with different Pt loadings.

B.8.: LSV curves of NF-MOF-Pt/C

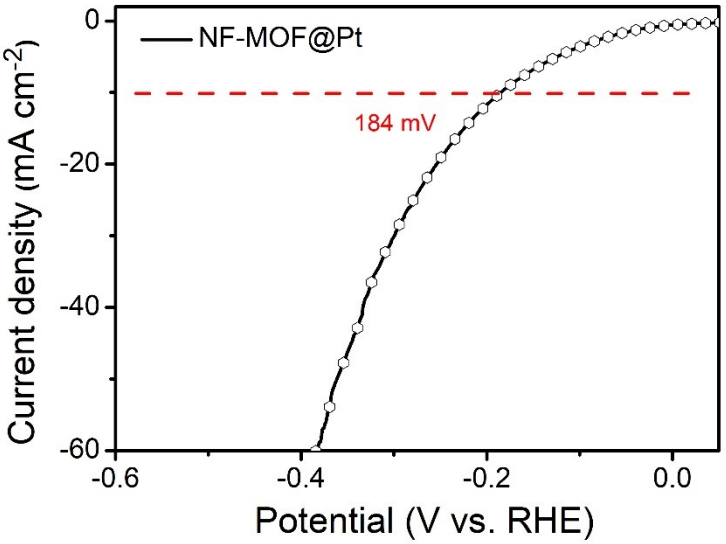

Figure S8: LSV curves of NF-MOF-Pt/C.

B.9.: CV curves of different catalysts at various scan rates

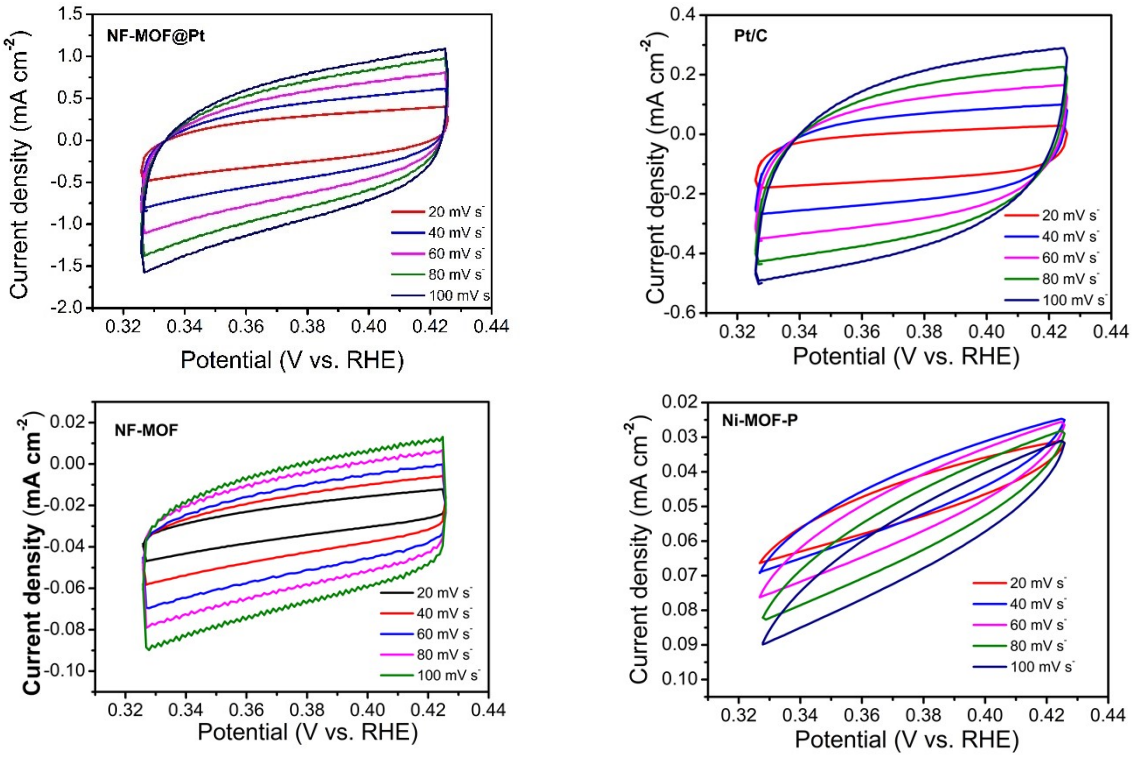

Figure S9: CV curves of different samples at various scan rates.

B.10.: ECSA normalized LSV curves of NF-Pt/C and NF-MOF@Pt

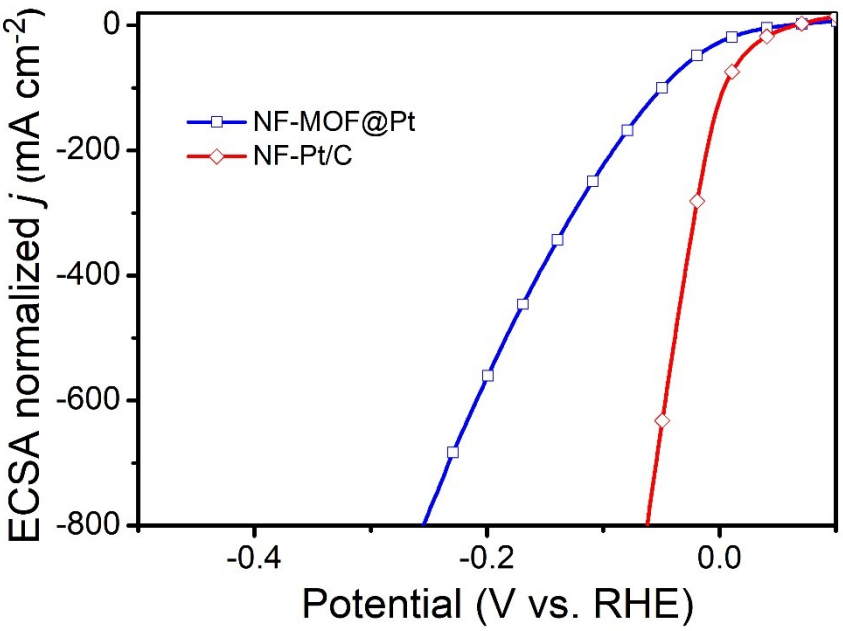

Figure S10: ECSA normalized LSV curves of NF-Pt/C and NF-MOF@Pt.

B.11.: EIS spectra of NF-MOF, NF-Pt/C, and NF-MOF@Pt electrodes

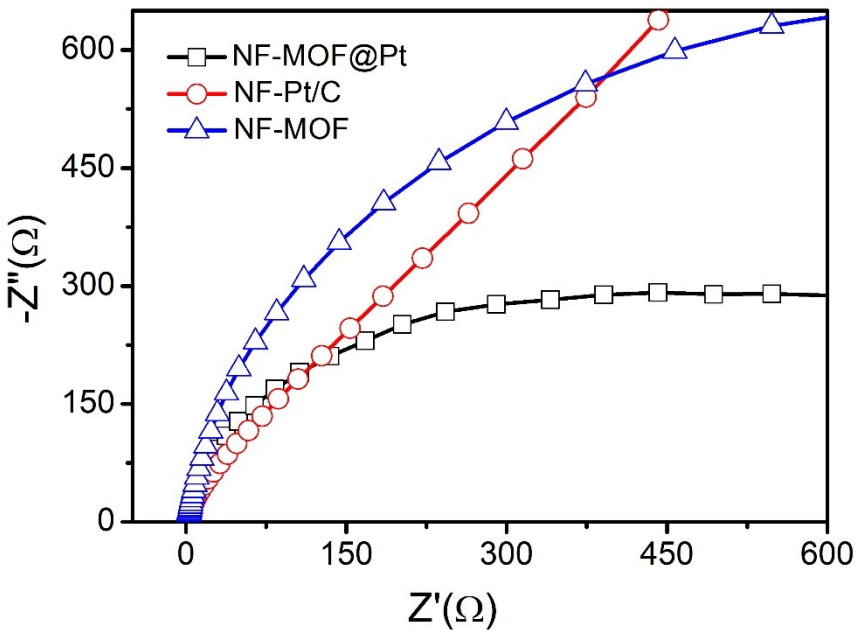

Figure S11: EIS spectra of NF-MOF, NF-Pt/C, and NF-MOF@Pt electrodes.

B.12.: SEM image of NF-MOF@Pt after stability test

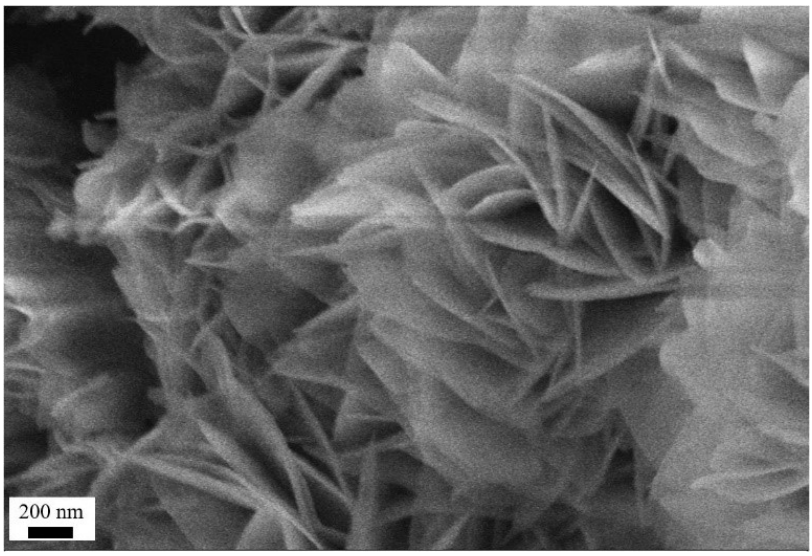

Figure S12: SEM image of NF-MOF@Pt after a 30 h HER test.

B.13.: XRD patterns of NF-MOF@Pt before and after a 30 h HER test

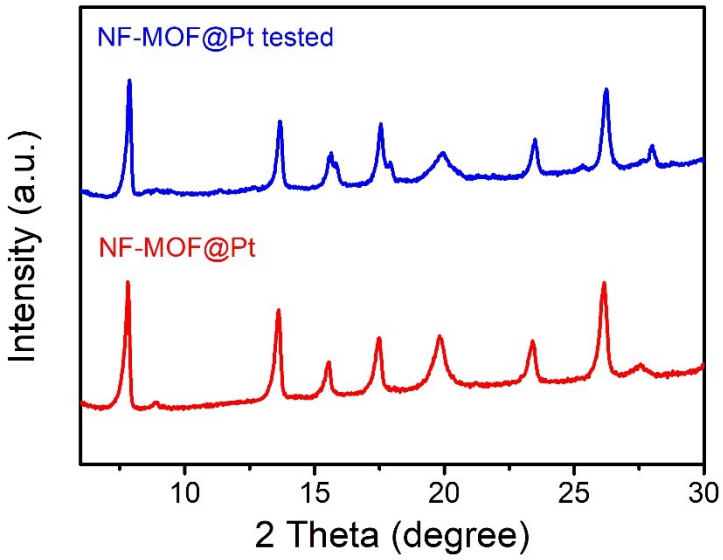

Figure S13: XRD patterns of NF-MOF@Pt before and after a 30 h HER test.

B.14.: ICP measurement

Table S1: Pt loadings of different NF-MOF@Pt samples.

Sample	Element	Weight percent of Pt (mg/kg)
Ni-MOF-NF-Pt-0.5	Pt	0.0224%
Ni-MOF-NF-Pt-1	Pt	0.0341%
Ni-MOF-NF-Pt-2	Pt	0.0644%
Ni-MOF-NF-Pt-5	Pt	0.1565%
Ni-MOF-NF-Pt-5-tested	Pt	0.1512%

B.15.: The overpotential and Tafel slope of different samples

Table S2: The summary of overpotentials and Tafel slopes of different samples.

Samples	Electrolyte	Overpotential (mV)	Tafel slope (mV dec^{-1})
NF-MOF@Pt-5	1 M KOH	28	52
NF-MOF@Pt-2	1 M KOH	77	67
NF-MOF@Pt-1	1 M KOH	222	89
NF-MOF@Pt-0.5	1 M KOH	260	106

B.16.: The overpotential and Tafel slope of different samples

Table S3: Summary of HER performance of the Pt-based electrocatalysts reported in the literature and this work.

Catalyst	Overpotential [mV]	Tafel slope [mV dec^{-2}]	Current density [mA cm^{-2}]	Electrolyte	Pt content [wt%]	Ref.
Pt-CoS_2/CC	24	82	10	1.0 M KOH	7.3	[45]
Pt_1/N-Ni/NF	33	24	10	1.0 M phosphate buffer saline	-	[46]
Pt-MoS_2	9	44	0.373	0.5 M H_2SO_4	11	[47]
$PtNC_3$-MXene	40	50.8	10	0.5 M H_2SO_4	-	[48]
LPWGA	42	30	10	0.5 M H_2SO	0.8	[49]
Pt-Ni	65	78	10	1.0 M KOH	11.5	[50]
CPt@ZIF-67	50	27.1	10	0.5 M H_2SO_4	5	[51]
Pt_{SA}-NT-NF	24	30	10	1.0 M phosphate buffer saline	1.76	[52]
Pt-GT-1	18	24	10	0.5 M H_2SO_4	0.5	[53]
Pt-NiFe LDH/CC	28	69	10	1.0 M KOH	1.56	[54]
Pt/GNs	25	33	10	0.5 M H_2SO_4	14.7	[55]
$Mo_2TiC_2T_x$-Pt_{SA}	30	30	10	0.5 M H_2SO_4	1.2	[56]
$Pt_1O_2C_1$	38	36	10	0.5 M H_2SO_4	0.27	[57]
Pt/Co_2P/Ni_2P/NF	75	64	10	1.0 M KOH	0.29	[58]
N,Pt-MoS_2	38	39	10	1.0 M KOH	1.2	[59]
NF-MOF-Pt	**28**	**52**	**10**	**1.0 M KOH**	**0.156**	**This work**